TIME- AND FREQUENCY-BASED INDEPENDENT EVALUATION OF QRST CANCELLATION TECHNIQUES FOR SINGLE-LEAD ELECTROCARDIOGRAMS DURING ATRIAL FIBRILLATION

Nicholas F. Price
Department of Electrical and Computer Engineering
University of Toledo
Toledo, OH 43607 USA
nicholaspri@gmail.com

Omer Berenfeld
Center for Arrhythmia Research
University of Michigan
Ann Arbor, MI 48107 USA
oberen@med.umich.edu

Vijay Devabhaktuni
Department of Electrical and Computer Engineering
The University of Maine
Orono, MN 04469, USA
vijay@maine.edu

Makarand Deo
Department of Engineering
Norfolk State University
Norfolk, VA 23504 USA
mdeo@nsu.edu

ABSTRACT

With the increased prevalence of atrial fibrillation (AF) –rhythm disturbances in heart's top chambers– there is growing interest in accurate non-invasive diagnosis of atrial activity to improve its therapy. A key component in non-invasive analysis of atrial activity is a successful removal of the ventricular QRST complexes from electrocardiograms (ECGs). In this study, we have developed a new approach for an objective and physiologically-based evaluation of QRST cancellation methods based on the power spectra of the AF. Three commonly used QRST cancellation methods were evaluated; namely, average beat subtraction, singular value cancellation, and principal component analysis. These methods were evaluated in time and frequency domains using a set of synthesized ECGs preserving the atrial-specific temporal and spectral properties. It was observed that the ABS method provided the best estimation when QRST morphological variability is low, while PCA produces an overall best estimate when a large QRST morphological variability is present.

Keywords: Electrocardiogram, Principal Component Analysis, QRST Cancellation, Atrial Fibrillation.

1 INTRODUCTION

An estimated 3 million Americans are currently afflicted by atrial fibrillation (AF), the most commonly sustained heart rhythm disorder, known as arrhythmia, in humans (Naccarelli et al. 2009). AF is associated with an increase in the risk of structural heart disease and a five-fold increase in stroke risk, both leading causes of death in the U.S. (Go et al. 2012).

There is a growing body of evidence demonstrating how characterization of the AF in the frequency domain increases our understanding of the disease and can improve its therapy (Berenfeld et al. 2011). Global assessment of the arrhythmia can be effectively performed through spectral analysis of the non-invasive electrocardiograms (ECGs) (Rodrigo et al. 2014). However, studying the spectral characteristics of AF

from ECGs is often difficult due to the much higher power of the ventricular activity (VA) components in the form of QRST complexes which mask the atrial activity (AA) in the ECG (see Figure 1 for an example). Therefore, in order to extract the AA information, it is imperative to eliminate the VA from the ECG.

Several QRST cancellation algorithms have been developed till date which exploit the spatiotemporal diversity using multiple leads (usually the standard 12-electrodes) of ECGs (Petrėnas et al. 2012). These techniques are powerful in analyzing the signals in persistent or permanent AF, which are more advanced and stable stages of the disease. However, their use is limited in the early stages of AF (paroxysmal AF) where the patients are usually monitored with a Holter system (Lee et al. 2012) or implanted devices in which only one to three leads might be available. The most common approaches to single-lead QRST cancellation include average beat subtraction (ABS) (R. Alcaraz and Rieta 2008), adaptive singular value QRST cancellation (SVC) (R. Alcaraz and Rieta 2008) and principal component based atrial activity estimation (PCA) (Castells et al. 2005).

Although these methods have been shown to eliminate visible VA from single-lead ECGs, their performance may be dependent on signal characteristics and is not validated against any independent measurement of the atrial activity to confirm that they retain the AA features in question. In fact, thus far there has been no systematic analysis comparing the performance of these frequently used cancellation algorithms and how their performance vary for single-lead ECG signal for varying activity data set precluding an *ad hoc* rationale for selection of an optimal algorithms. The main reason for lack of such comparison is the absence of an objective metric for quantitatively evaluate the performance of QRST cancellation.

We therefore develop and describe here a framework for comparison of QRST cancelation methods based on quantifying how well the cancelation method retains spectral properties of the AA that is extracted from non-VA segment of the ECG. Following the Welch principle, separated, VA-free, ECG segments retain the stationary power spectral characteristics of the AA and therefore can be used as a reference for the QRST cancelation method aiming at analysis of the AA in the frequency domain (Rodrigo et al. 2014). We focus here on comparing the performance of the three single-lead QRST removal algorithms under conditions of varying heart rate, duration, and morphological QRST variability. This comparison is performed by applying the algorithms to a controlled set of synthesized ECG signals derived from actual AF recordings with authentic and known time and frequency domain properties. The comparisons demonstrate that the effectiveness of each of these methods varies based on the characteristics of the signal, and therefore an *ad hoc* evaluation of the AA power spectrum and the QRST properties of the ECG signal may aid in selection of an appropriate VA removal method.

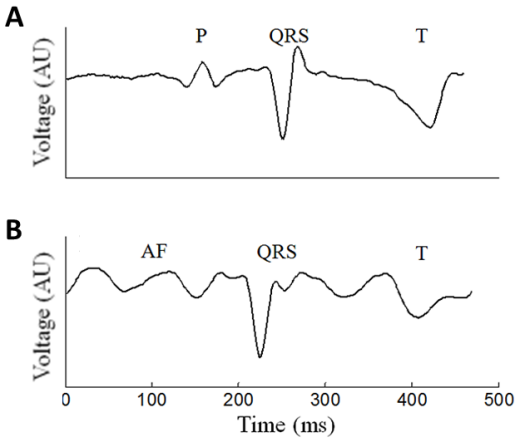

Figure 1. Examples of single-lead ECGs. A) During sinus rhythm, the lower amplitude P complex of the atrial activity is distinguishable from the QRS and T complexes of the ventricular activity. B) During AF, a lower amplitude atrial activity is present throughout the time-series and is masked at times by the larger amplitude ventricular activity (QRS and T complexes).

2 METHODS

2.1 Synthesizing ECG Data

The QRST cancelation algorithms were analyzed on single-lead ECG signals, with AA and VA components known *a priori*. The sources of both components were real surface ECG recordings in sheep with AF condition, collected via continuous cardiac rhythm monitoring using an implantable loop recorder (ILR) subcutaneously implanted in the sheep's sternum. All procedures were approved by the University of Michigan Committee on Use and Care of Animals and complied with National Institutes of Health guidelines. More details on the data collection can be found elsewhere (Filgueiras-Rama et al. 2012).

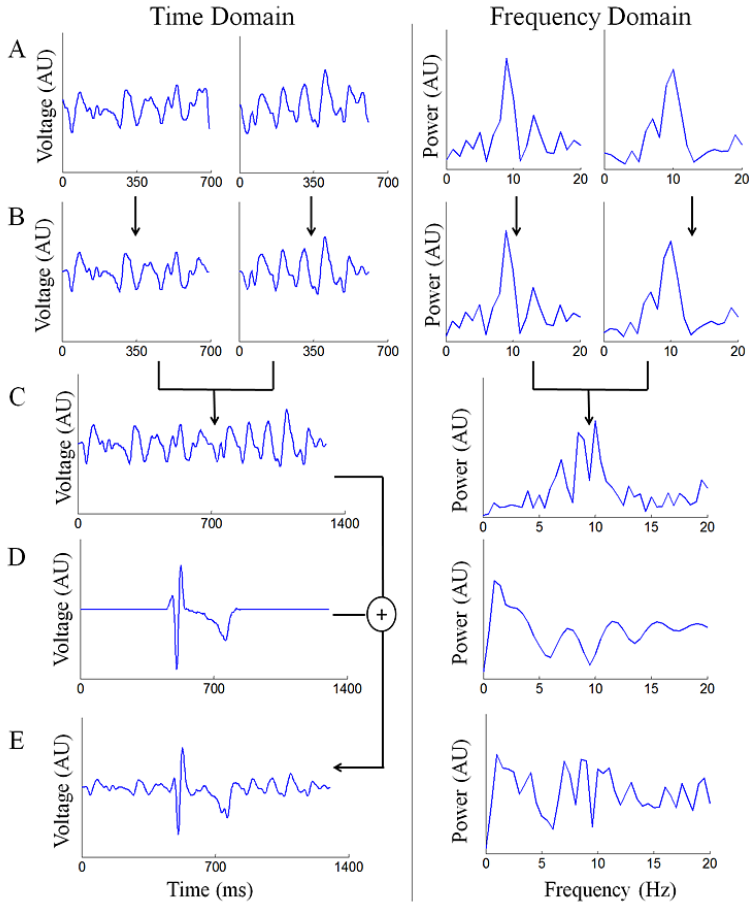

Figure 2. The process of synthesizing an ECG. The corresponding FFT-based power spectra of the traces are presented on the right side for each step of the process. A) Acquire ECG samples during AF and extract the QT segments. B) Remove any linear trends and taper the ends of each QT signal to zero by a Hanning window. C) Concatenate the processed AF segments into the synthetic AF signal. The AA-only power spectrum is seen on the right side. D) Extract QRST complexes from sinus rhythm ECGs. Then subtract the line which intersects the first and last samples of the QRST complex, such that both ends are equal to zero. Pad the ends and spaces between QRST complexes with a constant to form synthetic VA, of the same length as the synthetic AF signal. E) Add the synthetic VA to the synthetic AF signal to create the synthetic ECG.

A synthetic AF signal was constructed by manually splicing together TQ segments (the space between the end of the T-wave and the beginning of the Q waves) containing only atrial activity as illustrated in panels A-C of Figure 2. Each segment was set to a zero-mean value and tapered at both ends with half a Hanning window (spanning ~0.1 seconds). TQ segments were gathered to construct over four minutes of such AA.

Then QRST signals were constructed by QRST complexes from periods of sinus rhythm (normal ECG signals), with the P-wave excluded. The isoelectric line was set to zero at both ends and any linear trends were removed, as can be seen in Figure 2D. A set of 426 of these synthesized QRST complexes were collected and processed for the test data. After the QRST complexes were temporally arranged on the isoelectric line, the synthesized AA (Panel C) and VA (Panel D) were added together to form the synthesized ECG as seen in Figure 2E.

2.2 Evaluation Method

The synthesized QRST complexes were grouped together and compared using the Pearson correlation index (also known as cross-correlation). The Pearson correlation index is a means of comparing the similarity of two signals. If the index is 1, the signals are identical; if 0, then there is no correlation. For two zero-mean signals $\mathbf{s}_1$ and $\mathbf{s}_2$, the Pearson index is calculated as:

$$\rho = \frac{E[\boldsymbol{s}_1 \cdot \boldsymbol{s}_2]}{\sigma_1 \sigma_2} \tag{1}$$

where E[•] is the expectation operator and σ_1 and σ_2 are the standard deviations of $\mathbf{s}_1$ and $\mathbf{s}_2$ respectively. Variables $\mathbf{s}_1$ and $\mathbf{s}_2$ can also be chosen to be the subtracted and the reference AA signals, either in the time- or in the frequency-domain. The QRST variability is defined as the opposite of the QRST similarity:

$$\nu = 1 - |\rho| \tag{2}$$

where larger values for ν correspond to larger differences in QRST morphology. Figure 3 shows examples of how ν corresponds to morphological differences. With this information, test sets falling within specified ranges of QRST variability were created for the purpose of controlled testing of this parameter.

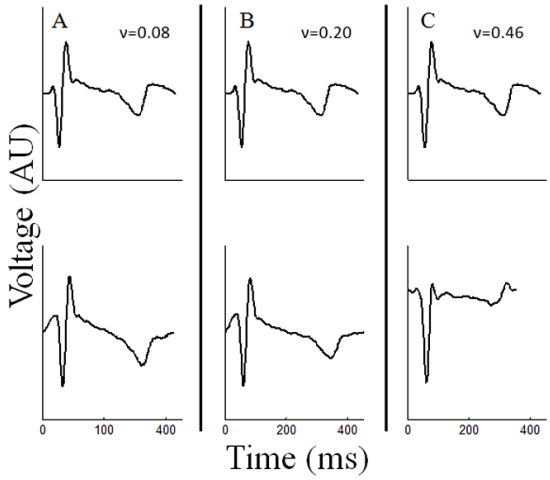

Figure 3. Examples of QRST variability from a sample reference QRST (top traces). A) Two QRST complexes in which ν=0.08, B) ν=0.20, C) ν=0.46.

2.3 Test Case Construction

The testing suite was implemented in MATLAB. When constructing a test case, the length (in seconds), the heart rate (in bpm), and the range of QRST complex variability were specified as parameters. Each synthesized ECG signal was linked to a copy of the known atrial and ventricular activity from which it was constituted. The fast Fourier transform (FFT) was computed for the AA trace so the AA estimation produced by each QRST removal algorithm could be compared to the known AA both in the time domain and in the frequency domain.

2.4 Test Parameters

The methods being tested were evaluated based on the accuracy of the AA estimates they produced – i.e. how similar they were to the known, true, AA in both the time and frequency domain as measured in terms of the Pearson correlation index (Eq. 1). Besides the type of algorithm being used, the main independent variable was the average variability between the QRST complexes within each test case. The secondary and tertiary independent variables were the length of the test case signal and the heart rate, respectively. The five bins of QRST variability were: v = 0.05±0.05, 0.15±0.05, 0.25±0.05, 0.35±0.05, and 0.45±0.05. The four categories of signal length were 5 seconds, 10 seconds, 15 seconds and 20 seconds. The types of heart rates tested were 60 bpm, 80 bpm, 100 bpm, and 120 bpm. All 80 combinations were tested against the three algorithms, with 100 test cases each.

2.5 QRST Cancelation Algorithms

Average Beat Subtraction (ABS): There are multiple variations on ABS,(Alcaraz and Rieta 2008) but the most generic form of ABS was implemented which generates a template for VA by averaging the QRST complexes in the signal. Because the AA is assumed to be independent from the VA, it cancels out in the averaging. After the template was derived, it was subtracted from the original signal at each QRST location such that the R-peaks are aligned.

Singular Value Cancellation (SVC): The SVC algorithm was implemented as defined in.(Alcaraz and Rieta 2007) The QRST complexes in the trace being tested were arranged into the column vectors of a matrix **X** (i.e. $\mathbf{X}=[\mathbf{x}_1, \mathbf{x}_2, \ldots, \mathbf{x}_n]$, where $\mathbf{x}_i$ are temporally aligned vectors of QRST complexes), on which singular value decomposition was performed:

$$\mathbf{X}=\mathbf{U}\mathbf{S}\mathbf{V}^{\mathrm{T}}.$$

The matrix **U** is an unitary matrix containing eigen vectors of **X**, **S** is a diagonal matrix containing eigen values or singular values of **X**, sorted in a descending order, and **V** is an upper diagonal matrix. The matrices **U** and **S** were then re-multiplied $\mathbf{C}=\mathbf{U}\mathbf{S}$, so that **C** is a matrix of the principal components. The first principal component was selected as a template and was then scaled by a factor of QR_i/QR_t where QR_i is the difference in amplitude between the Q-peak an R-peak of i^{th} QRST complex and QR_t is the same measurement, but from the template. After scaling, the SVC template was subtracted from the original signal in the same manner as in ABS.

Principal Component Analysis (PCA): The PCA algorithm, like SVC, uses principal components to derive a template (Castells et al. 2005). However, instead of simply scaling the first principal component based on the QR difference, the PCA algorithm recombines a subset of the principal components that are most associated with VA. This makes PCA unique among the other three algorithms in that the number of principal components used to construct the VA template can be an adjustable parameter. For illustrative purposes, suppose the principal components of observation matrix **X** can be obtained through linear transformation **W**:

$$\mathbf{P} = \mathbf{W}\mathbf{X}^{T} \tag{3}$$

where **P** is a matrix in which the row vectors are the principal components ordered by variance. Because the VA is the dominant feature, the first one or more principal components can be assumed to be most associated with VA. The subsequent components can then be assumed to correspond with AA and noise. By isolating only those principal components associated with VA in a matrix $\mathbf{P}_V$ and multiplying it by the associated columns of the inverse transformation matrix $\mathbf{W}^{-1}$, a VA template can be generated for each QRST complex from the original observation matrix.

$$\boldsymbol{T}_V = \boldsymbol{W}^{-1}\boldsymbol{P}_V \tag{4}$$

The matrix $\mathbf{T}_V$ contains VA templates for each of the QRST complexes in the test case, which are then subtracted from the originating trace.

While this makes the PCA method more flexible, it necessitates that several sets of tests are needed to truly gauge the effectiveness of the PCA algorithm. Optimal PCA was defined as the version of the PCA algorithm in which the optimal number of components (n) was used in every case. This was achieved by applying the algorithm to the test with $n = 1$ first, and then reapplying the algorithm with incrementally increasing values of n until the results ceased improving (as defined as the ρ value between the AA estimate and the known AA). This was considered the optimal value of n, which was adopted for optimal PCA's test results. The PCA algorithm was also applied to the same test cases using fixed values of n. These tests were performed for $n = 1, 2, 3, 4$, and then 5. Each of these was defined as one-component PCA, two-component PCA, three-component PCA, etc. Unless stated otherwise, optimal PCA was used as the test results for the PCA algorithm.

3 RESULTS

Figure 4 shows the outcome of all the three methods under consideration applied to a synthesized AF trace. The sample synthesized ECG, including both VA and AA, is shown in Figure 4A along with its corresponding power spectrum in Figure 4B. Comparing the 3 QRST removal methods with the true AA signal (Figure 4I) shows a general reduction of the VA, but with varying resulted estimated AA between the methods. Information on the QRST reduction in the frequency domain can further help in evaluating the performance of these 3 methods. By comparing Figure 4J with 4B we realize that the VA contributes spectral power primarily in frequencies below the dominant frequency (DF) peak at about 9 Hz. Although all three methods were able to reduce the power of QRST segments, their effectiveness in extracting precise AA information and reproducing the DF of the AA (Figure 4J) was variable. Thus, we can use the comparisons between the power spectra of the estimated AA with the power spectrum of the true AA that can be obtained from atria-only segments in ECGs as a measure for the performance of the 3 QRST cancellation algorithms.

The performance of the PCA method was dependent on the number of components used to extract the QRST information. Figures 4G and 4H show the extracted information using the PCA method applied to a sample ECG trace with two principal components. An example of the first 8 principal components of an ECG is shown in Figure 5. As mentioned above, because VA is a dominant feature in the QRST complex, it is assumed that VA components will be the most primary. In the case of Figure 5, the morphological characteristics and power of the first two components suggest that indeed they are associated with VA. The next three components (components three, four and five) appear to mostly be associated with AA. The higher components are less powerful and are presumably associated with noise. As the goal here is to eliminate VA in the form of QRST segments, principal components only up to the 3rd order were considered.

Figure 6 shows the quality of estimation of VA using one-component, two-component, and three-component PCA methods. As can be seen from Figure 6A, the optimal number of principal components increased as the average QRST morphological variability was increased. The traces with the lowest variability in QRST complexes most often needed only one principal component for optimal QRST cancellation. This increased to three principal components as the average QRST variability was increased to 0.45 ± 0.05. The effects of two other parameters—namely, length of the signal and heart rate—were also studied on the performance of the QRST cancellation methods (see Figure 7). It was observed that all else unchanged, the greater the length of the signal, the better all algorithms performed (Figure 7A). On the other hand, the overall performance of all three methods worsened with the increase in heart rate (Figure 7B).

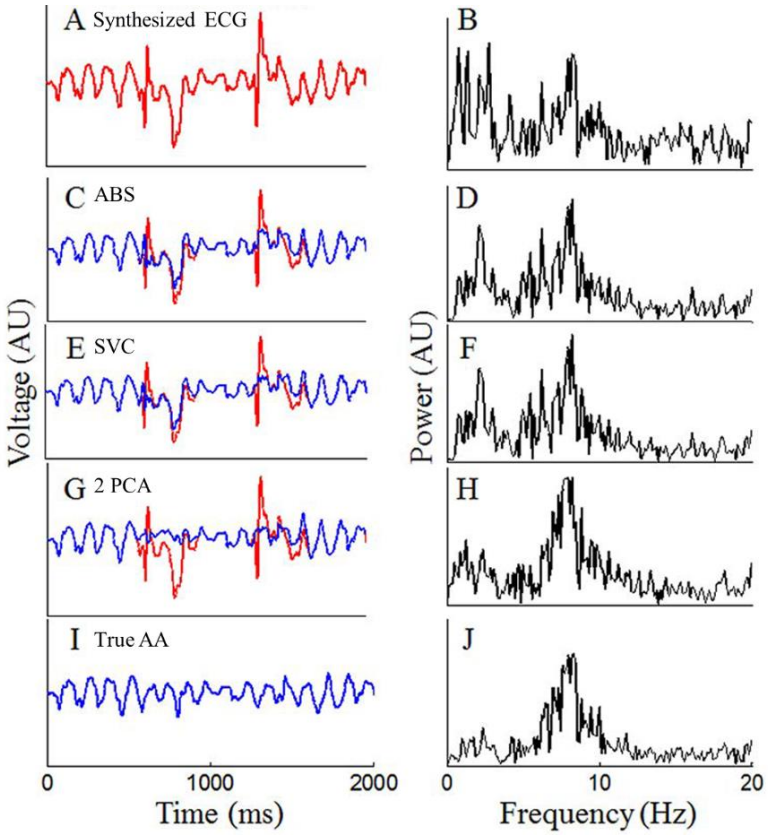

Figure 4. An example of all three QRST removal methods applied to a sample AF single-lead ECG recording A) Synthesized ECG segment (red) with both atrial and ventricular activity consisting of 2 QRST complexes along with B) corresponding power spectrum. C) The estimated AA (blue) using the ABS algorithm superimposed on the ECG from A (red) with D) corresponding power spectrum. E) The estimated AA (blue) using the SVC algorithm superimposed on the ECG from A (red) with F) corresponding power spectrum. G) The estimated AA (blue) using the two-component PCA algorithm superimposed on the ECG from A (red) with H) corresponding power spectrum. I) The true AA (blue) of the synthesized ECG with J) corresponding power spectrum.

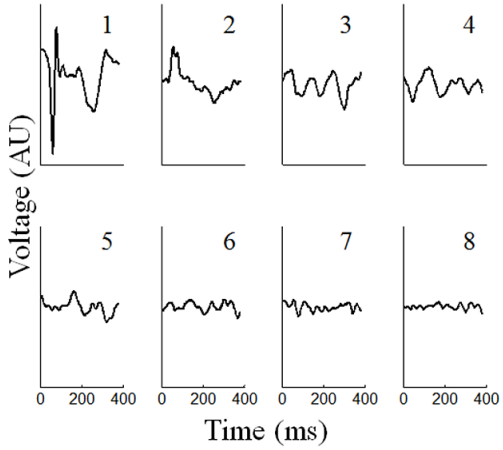

Figure 5. The first eight principal components derived using the PCA method applied to a sample ECG trace. The first two components describe VA, followed by the next 3 providing AA information, whereas the last 3 describing mostly noise.

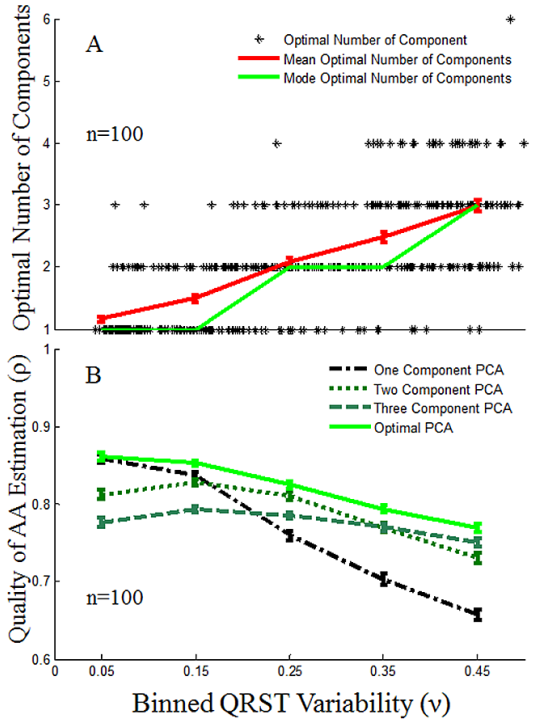

Figure 6. A) The optimal number of principal components for the PCA and the QRST variability indices of their associated traces. B) The quality of estimation in the time domain of the PCA method using one component, two components, three components and the optimal number of components on the same data set as panel A.

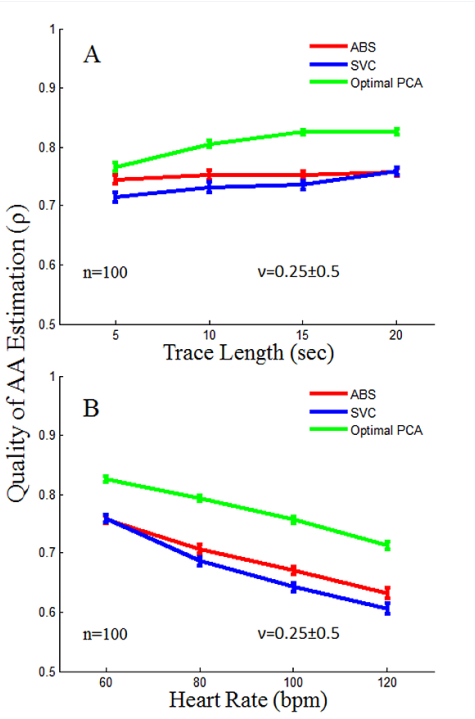

Figure 7. Quality of estimation for the three QRST cancellation algorithms for traces in which the QRST variability is 0.25±0.05 but with variable lengths and heart rates. A) Compares quality of estimation for traces with different lengths and a heart rate of 60 bpm. B) Compares quality of estimation for traces with different heart rates and a length of 20 sec.

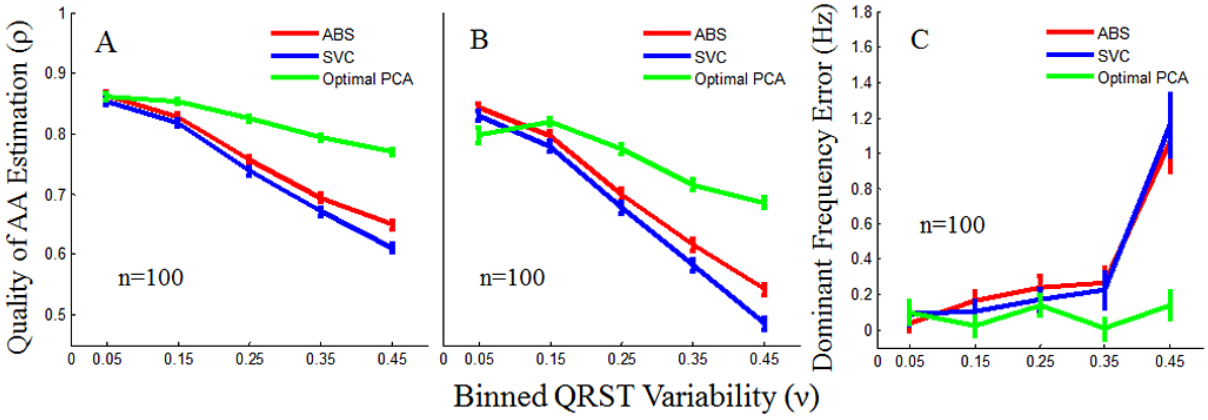

Figure 8. Performance of the three QRST cancellation methods with varying signal variability. Quality of estimation (ρ) for ABS, SVC and Optimal PCA was assessed using synthesized traces of 20 seconds long, 60 bpm heart rate and varying QRST variability (ν) in A) time domain and B) Frequency domain as calculated by the fast Fourier transform. C) Mean error of the estimated dominant frequency as calculated using the same data set as in panel A and B.

Figure 8A and 8B shows the performance of the three QRST cancellation methods with increasing morphological QRST variability in the signals, assessed in time and frequency domains, respectively. The optimal PCA algorithm provided the most accurate AA estimates, except for situations where the average QRST variability was very low. The ABS and SVC methods were able to obtain better AA estimates than the optimal PCA for the low QRST variability when the frequency domain results are considered, but their effectiveness was monotonically decreased as QRST variability was increased. This trend was evident in both time (panel A) and frequency (panel B) domains. Panel C plots the mean error in estimated DF for the same three methods on the same data set used in panels A and B. The optimal PCA provided better DF estimates over the considered range of QRST variability.

4 DISCUSSION

This paper compares the performance of single-lead QRST cancellation methods for the first time against preserved, atrial-only spectral characteristics. The extraction of the time series and power spectra of the atria-only activity during AF in this study serves as an independent solid reference for performance comparison of the different cancellation methods. The results contribute *ad hoc* solutions for given QRST characteristics, which can be used by future researchers as a guide for picking the best QRST cancellation algorithm for processing their data. Specifically, the results indicate that PCA is most effective when there is a high degree of variability between QRST complexes, but ABS is superior when the QRST complexes in the signal are very similar. The performance of ABS degrades with increasing variability because it uses all the ECG complexes in the signal trace to generate a VA template. Other variants of ABS have been proposed to address this limitation by combining the information from adjacent leads (Stridh and Sörnmo 2001) or by separately processing the T waves (Mathieu Lemay et al. 2007). However, their extension to the single-lead signals has not been effective. On the other hand, the PCA utilizes a set of base functions to cancel the VA in multiple orthogonal components instead of cancellation from a single template.(Castells et al. 2005) Therefore PCA is much more effective in removing the VA from signals with very high degree of variability. Furthermore, the performance of the PCA method for analysis of AF is improved by determining the optimal number of components. However, this requires knowing the actual AA *a priori* and so it may not be practical in most real-world scenarios. Nonetheless, the results obtained using fixed number of components (e.g. Fig. 6) may give some guidelines to estimate the optimal number of components.

In this study, we analyzed in detail the performance of the three algorithms being tested under different, quantifiable QRST variability circumstances. This independent performance comparison was performed on benchmark data and provides unbiased results given a variety of scenarios. This comparison is important, as previous results may be biased based on choice of method on particular data. For example, it was implied in (Alcaraz and Rieta 2007) that the SVC method was superior to the PCA method. That is, it was reported to produce an average $\rho = 0.92 \pm 0.07$ between the actual and estimated AA of their synthesized ECGs while citing that (Castells et al. 2005) reported only $\rho = 0.774 \pm 0.106$. Given how much the performance of QRST cancellation method can be affected by the varying ECG signal characteristics, as demonstrated in this work, it is imperative to consider all possible scenarios to make valid comparisons. Thus, the presented study provides a framework for how performance of QRST cancellation algorithms can be compared in the future.

5 CONCLUSION

This study provides a novel framework for spectral-based evaluation for single-lead ECG QRST removal methods, especially in the context of atrial arrhythmias. Using a multi-segment average power spectrum of the AA activity we provide an objective evaluation criterion for the quality of the QRST removal. The ABS algorithm provided the most accurate AA estimation when the difference between sequential QRST morphologies was minor. However, when the QRST morphology was varied between beats, both SVC and ABS left enough ventricular residual signals to dramatically decrease the quality of their AA estimates. On the other hand, the PCA algorithm was better able to adapt to QRST morphological variability, and was

usually able to do so using only two or three principal components. However, using two components on traces with only small differences between QRST complexes removes important AA components from the estimation. Thus, when performing QRST removal on single-lead ECG traces, the best strategy found is the PCA method using just enough principal components to remove ventricular artifacts from the signal. The findings promote an unbiased validation and comparison of current QRST removal techniques, with aims to best characterize AF in the frequency domain.

ACKNOWLEDGEMENT

We thank Drs. David Rama-Filgueiras, Raphael Martins, and Steven Ennis for the ECG data from which the test sets were derived and the Center for Arrhythmia Research at the University of Michigan for making the data available for this study. This work was supported in part by grants from the Leducq Foundation; National Heart, Lung, and Blood Institute grants [P01-HL039707 and P01-HL087226]; the Gelman Award from the Cardiovascular Division at the University of Michigan; and the Coulter Program Award from the Dept. of Biomed Eng. at the University of Michigan.

REFERENCES

Alcaraz, R., and J. J. Rieta. 2008. "Optimal Beat Selection Study for QSRT Cancellation Methods in the ECG of Atrial Fibrillation." *Computers in Cardiology* vol. 35, pp. 1045–48.

Alcaraz, R., and J.J. Rieta. 2007. "Adaptive Singular Value QRST Cancellation for the Analysis of Short Single Lead Atrial Fibrillation Electrocardiograms." *Computers in Cardiology* vol. 34, pp. 513–16.

Atienza, F., J. Almendral, J. Jalife, S. Zlochiver, R. Ploutz-Snyder, E. G. Torrecilla, A. Arenal, J. Kalifa, F. Fernández-Avilés, and O. Berenfeld. 2009. "Real-Time Dominant Frequency Mapping and Ablation of Dominant Frequency Sites in Atrial Fibrillation with Left-to-Right Frequency Gradients Predicts Long-Term Maintenance of Sinus Rhythm." *Heart Rhythm : The Official Journal of the Heart Rhythm Society* vol. 6 (1), pp. 33–40. https://doi.org/10.1016/j.hrthm.2008.10.024.

Berenfeld, O., S. Ennis, E. Hwang, B. Hooven, K. Grzeda, S. Mironov, M. Yamazaki, J. Kalifa, and J. Jalife. 2011. "Time- and Frequency-Domain Analyses of Atrial Fibrillation Activation Rate: The Optical Mapping Reference." *Heart Rhythm : The Official Journal of the Heart Rhythm Society* vol. 8 (11), pp 1758–65. https://doi.org/10.1016/j.hrthm.2011.05.007.

Castells, F., C. Mora, J. J. Rieta, D. Moratal-Pérez, and J. Millet. 2005. "Estimation of Atrial Fibrillatory Wave from Single-Lead Atrial Fibrillation Electrocardiograms Using Principal Component Analysis Concepts." *Medical & Biological Engineering & Computing* vol. 43 (5), pp. 557–60. https://doi.org/10.1007/BF02351028.

Filgueiras-Rama, D., N. F. Price, R. P. Martins, M. Yamazaki, U. R. Avula, K. Kaur, J. Kalifa, et al. 2012. "Long-Term Frequency Gradients during Persistent Atrial Fibrillation in Sheep Are Associated with Stable Sources in the Left Atrium." *Circulation. Arrhythmia and Electrophysiology* vol. 5 (6), pp. 1160–67. https://doi.org/10.1161/CIRCEP.111.969519.

Go, A. S., D. Mozaffarian, V. L. Roger, E. J. Benjamin, J. D. Berry, W. B. Borden, D. M. Bravata, et al. 2012. "Heart Disease and Stroke Statistics--2013 Update A Report From the American Heart Association." *Circulation* vol. 127 (1), pp e6-245. https://doi.org/10.1161/CIR.0b013e31828124ad.

Guillem, M. S., A. M. Climent, J. Millet, Á. Arenal, F. Fernández-Avilés, J. Jalife, F. Atienza, and O. Berenfeld. 2013. "Noninvasive Localization of Maximal Frequency Sites of Atrial Fibrillation by Body Surface Potential Mapping." *Circulation. Arrhythmia and Electrophysiology* vol. 6 (2), pp. 294–301. https://doi.org/10.1161/CIRCEP.112.000167.

Lee, J., M. Song, D. Shin, and K. Lee. 2012. "Event Synchronous Adaptive Filter Based Atrial Activity Estimation in Single-Lead Atrial Fibrillation Electrocardiograms." *Medical & Biological Engineering & Computing* vol. 50 (8), pp 801–11. https://doi.org/10.1007/s11517-012-0931-7.

Lemay, M., V. Jacquement, A. Forclaz, J.M. Vesin, and L. Kappenberger. 2005. "Spatiotemporal QRST Cancellation Method Using Separate QRS and T-Waves Templates." *Computers in Cardiology* vol. 32, pp. 611–14.

Lemay, M., J. Vesin, A. van Oosterom, V. Jacquemet, and L. Kappenberger. 2007. "Cancellation of Ventricular Activity in the ECG: Evaluation of Novel and Existing Methods." *IEEE Transactions on Bio-Medical Engineering* vol. 54 (3), pp. 542–46. https://doi.org/10.1109/TBME.2006.888835.

Llinares, R., J. Igual, and J. Miro-Borras. 2010. "A Fixed Point Algorithm for Extracting the Atrial Activity in the Frequency Domain." *Computers in Biology and Medicine* vol. 40, pp. 943–49.

Naccarelli, G. V., H. Varker, J. Lin, and K. L. Schulman. 2009. "Increasing Prevalence of Atrial FIbrillation and FLutter in the United States." *American Journal of Cardiology* vol. 104 (11), pp. 1534–39.

Petrėnas, A., V. Marozas, L. Sörnmo, and A. Lukosevicius. 2012. "An Echo State Neural Network for QRST Cancellation during Atrial Fibrillation." *IEEE Transactions on Biomedical Engineering* vol. 59 (10), pp. 2950–57. https://doi.org/10.1109/TBME.2012.2212895.

Petrutiu, S., J. Ng, G. M. Nijm, H. Al-Angari, S. Swiryn, and A. V. Sahakian. "Atrial Fibrillation and Waveform Characterization. A Time Domain Perspective in the Surface ECG." *IEEE Engineering in Medicine and Biology Magazine : The Quarterly Magazine of the Engineering in Medicine & Biology Society* vol. 25 (6), pp. 24–30.

Rieta, J. J., F. Castells, C. Sánchez, V. Zarzoso, and J. Millet. 2004. "Atrial Activity Extraction for Atrial Fibrillation Analysis Using Blind Source Separation." *IEEE Transactions on Bio-Medical Engineering* vol. 51 (7), pp. 1176–86. https://doi.org/10.1109/TBME.2004.827272.

Rodrigo, M., M. S. Guillem, A. M. Climent, J. Pedrón-Torrecilla, A. Liberos, J. Millet, F. Fernández-Avilés, F. Atienza, and O. Berenfeld. 2014. "Body Surface Localization of Left and Right Atrial High-Frequency Rotors in Atrial Fibrillation Patients: A Clinical-Computational Study." *Heart Rhythm : The Official Journal of the Heart Rhythm Society* vol. 11 (9), pp. 1584–91. https://doi.org/10.1016/j.hrthm.2014.05.013.

Stridh, M., and L. Sörnmo. 2001. "Spatiotemporal QRST Cancellation Techniques for Analysis of Atrial Fibrillation." *IEEE Transactions on Biomedical Engineering* vol. 48 (1), pp. 105–11. https://doi.org/10.1109/10.900266.

AUTHOR BIOGRAPHIES

NICHOLAS F. PRICE was a MS student in the Department of Electrical and Computer Engineering at The University of Toledo, Toledo, OH. He is currently working at Intel Corporation. His email address is nicholaspri@gmail.com.

OMER BERENFELD is a Professor of Internal Medicine and Biomedical Engineering at University of Michigan at Ann Arbor, MI. Dr. Berenfeld's research expertise are in cardiac arrhythmia mechanisms and numerical modeling of cardiac electrophysiology. His email address is oberen@med.umich.edu.

VIJAY DEVABHAKTUNI is the Norman Stetson Professor and Chair of Electrical and Computer Engineering at The University of Maine, Orono, MN. His research interests include modeling of RF microwave circuits and Artificial Neural Networks. His email address is vijay@maine.edu.

MAKARAND DEO is an Associate Professor in the Department of Engineering at Norfolk State University, Norfolk, VA. His research interests include multiscale modeling and simulation of cardiac electrophysiology and biosensing systems. His email address is mdeo@nsu.edu.